18

FERMILAB
AUG 1 1997
LIBRARY

IUCAA -16/97

February 97

Radiation Pressure and Stability of Interferometric Gravitational Wave Detectors

Fermilab Library
0 1160 0057574 0

IUCAA-16-97

By

Vijay Chickarmane
Sanjeev V. Dhurandhar
Roland Barillet
Patrice Hello
Jean-Yves Vinet

Inter-University Centre for Astronomy and Astrophysics

An Autonomous Institution of the University Grants Commission

Preprint Request (Please quote the preprint number)
email : preprn@iucaa.ernet.in
Fax : 0212-350760
Post : IUCAA, Post Bag 4, Ganeshkhind, Pune 411 007, India

Radiation pressure and stability of interferometric gravitational wave detectors

Vijay Chickarmane, Sanjeev V. Dhurandhar
Inter University Centre for Astronomy and Astrophysics
Postbag 4, Ganeshkind, Pune 411007 (India)

Roland Barillet
(Virgo Collaboration)
Laboratoire de l'Horloge Atomique
Université Paris-Sud, 91405 Orsay (France)

Patrice Hello
(Virgo Collaboration)
Laboratoire de l'Accélérateur Linéaire
Université Paris-Sud, 91405 Orsay (France)
, LAL

Jean-Yves Vinet
(Virgo Collaboration)
Laboratoire d'Optique Appliquée
Ecole polytechnique, Ecole Nationale Supérieure de Techniques Avancées
91761 Palaiseau (France)

The effect of radiation pressure on the stability of Fabry - Perot (FP) cavities with hanging mirrors is investigated. Such cavities will form an integral part of the laser interferometric gravitational wave detectors which are being constructed around the globe. The mirrors are hung via a pendulum suspension and are locked by servo-controls. We assume a realistic servo-control transfer function which satisfies the standard stability criteria. We find that, for positive offsets from the resonance of the cavity, the system is stable, as in the non servoed case. However, we show that, for negative offsets, instabilities can occur, although the servo system has the effect of increasing the instability threshold, as compared with the non-servoed case. Condition for stability is finally given, involving the finesse of the cavity, the input power, the mass of the mirrors, the servo gain and the phase detuning from perfect resonance. Gravitational-wave detectors with arm cavities having a finesse as low as about 200 could exhibit instabilities. Some implications for the locking of these detectors are finally given.

I. INTRODUCTION

Considerable progress has been made over the past few decades in the development of laser interferometric gravitational wave detectors. These detectors which are built on the lines of very large Michelson interferometers are very sensitive to length changes in the two arms which may be due to incident gravitational waves [1,2]. Each arm of the detector comprises a Fabry-Perot cavity made of a corner mirror and an end mirror suspended as a pendulum. An incident gravitational wave modulates the phase acquired by the propagating beam of light in the two arms of the interferometer in antiphase. This can be observed as a time dependent variation in the intensity at the photodetector. Various noise sources plague the interferometer such as the seismic noise, the thermal noise, shot noise etc [3]. But in the high frequency regime of the band-width of the detector it is the photon shot noise that dominates the noise spectrum. The photon shot noise falls off inversely as the square-root of the power and therefore for this purpose high input powers are conducive for obtaining high sensitivities. The power recycling technique [4,5] serves to increase the laser power of the light in the interferometer and hence makes it more sensitive. As a result of the recycling technique, the incident powers are of the order of the kW and could easily increase to few hundred kW or even a MW in the advanced detectors envisaged. The high powers incident on the mirrors can disturb the delicate balance in these highly tuned sensitive instruments and could either drive the cavity out of resonance or produce time dependent effects such as instabilities. Thermal absorption of laser power within the mirror can heat up the mirror, deforming it and effectively changing the length of the cavity. If the mirrors are freely hanging, the effect of the radiation pressure on the mirrors is important and must be taken into account in the design of the interferometric system.

This problem has already been considered by several authors. Dorsel et al. [6] first studied experimentally the occurence of multistability due to the radiation pressure force. The basics of multistability have been then established theoretically in [7]. Using more rigorous techniques, Tourrenc and collaborators [8] considered the stability of a cavity with freely suspended mirrors with time delay effects. They also did a numerical investigation of the mirror motion in

the unstable regime. Meers and MacDonald [9] also considered this problem in the context of proposed gravitational detectors which included recycling techniques. They included a crude servo system modeled simply as a damped harmonic oscillator which they found could stabilize the system under certain conditions. In this paper we consider a realistic servo system for the large scale detectors underway. The radiation pressure pushes on the mirrors modifying the length of the cavity which changes the incident power on the mirrors which in turn changes the radiation pressure. The coupling to the power is nonlinear and hence one may expect instabilities [6,8,9]. In this paper we will only consider the effects of radiation pressure pushing on the mirrors. We only wish to comment here that thermal effects are also relevant when high powers are employed since the mirror can be deformed due to thermo-elastic effects [11]. It has been shown that although the operating point of the cavity can be altered, no instabilities in the form of oscillations are observed [12].

In the present analysis we include the effect of the servo-system since the mirrors in the actual cavities will be locked by the servo. We have used the servo-control transfer function given by Caron et al. [14] in incorporating the effect of the servo. We proceed as follows: First we obtain the transfer function connecting the time dependent length of the cavity to the power which follows these changes. The method we use in deriving this last result is closely related to the one used in [9]. We find that at frequencies much smaller than the storage time-scale of the cavity, the power follows essentially the static Fabry-Perot curve and only when the changes in the cavity length are rapid enough, the response is nontrivial as given by the transfer function. The instantaneous radiation pressure force is just proportional to the power, as a function of the detuning. The radiation pressure force and the servo force act together on the suspended mirror. In effect, we obtain a feedback loop and thus a characteristic equation for the mirror displacement. The roots of this equation determine the stability of the system and they essentially depend on the phase offset δ of the operating point, the finesse of the cavity and the input power. We find that for $\delta > 0$ the system is stable. For $\delta < 0$, but chosen within the line width, for a given finesse and above a certain critical power the cavity becomes unstable. The critical power depends on the servo gain. If no servo is employed the critical power is small but nonzero owing to the restoring force of the pendulum suspension.

II. THE TRANSFER FUNCTION CONNECTING CAVITY LENGTH TO THE STORED POWER

In this section we derive the relation between the change in the stored power as the length of the cavity varies in time. We consider only small changes in the length of the cavity so that the relation is linear and can be expressed via a transfer function. In order to do this we first need to calculate the intra-cavity fields and from these the intra-cavity power.

We consider a single mirror, the end mirror, suspended as a pendulum, which is acted upon by the radiation pressure, the gravity and the servo forces. In the static limit the radiation pressure, the restoring force of the pendulum and the servo force balance each other to produce an equilibrium position for the mirror. We examine the stability of the system about the equilibrium position (or one of the positions) by considering how a small motion of the mirror affects the intra-cavity power. In order to do this we must first investigate how the electric field changes as the mirror is moved. The next section deals with this issue.

A. The electric fields

Let the length of the cavity be modulated at a particular frequency ω. Obtaining the response at a single frequency is equivalent to calculating the impulse response of the cavity to a change in its length. This motion of the mirror modulates the phase of the light in the cavity. If the incident laser frequency (carrier) is ω_l, then at least two sidebands are produced at frequencies $\omega_l \pm \omega$. These sidebands beat with the carrier to give rise to an intensity change which exerts time dependent radiation pressure on the end mirror. Let the cavity be aligned along the $x-$axis and the corner mirror and end mirror amplitude reflectivity be r_0 and r_1 respectively. The total round trip travel time for light is $\tau = 2l/c$, where l is the length of the cavity and c is the speed of light. The carrier wave ($\omega_l = 2\pi c/\lambda$) acquires a phase due to a small motion $\delta x(t) = x_o \sin \omega t$,

$$\delta\phi(t) = 2k\delta x(t) = 2kx_o \sin \omega t, \tag{1}$$

where the wavevector $k = 2\pi/\lambda$. In this expression of the small phase shift, we consider the wavelength as a constant, the mechanical frequency being small compared to the optical one, the sidebands are considered to have the same wavelength. Referring to Figure 1, the equations for the electric fields at the corner mirror are,

$$E_1(t) = t_0 E_0(t) + r_0 E_2(t), \tag{2}$$

$$E_2(t) = r_1 E_1(t-\tau)e^{-i\delta\phi(t-\tau/2)}. \tag{3}$$

The sign convention for reflection is chosen such that a positive sign is associated with a reflection from the inner surfaces, whereas a negative sign is associated for the outer surfaces. In Eq.(3), we see that the extra phase change acquired by the light (due to the moving mirror) which arrives at a certain time at the corner mirror, depends on the motion of the mirror at a delayed time, the delay being precisely half the round trip travel time. Substituting for E_2 in Eq.(2) one obtains,

$$E_1(t) = t_0 E_0(t) + r_o r_1 E_1(t-\tau)e^{-2ikx_o \sin\omega(t-\frac{\tau}{2})}. \tag{4}$$

Taking Fourier transforms of the electric fields and assuming that the mirror motion is much smaller than a wavelength, we expand to first order in $\epsilon \equiv kx_o$. Denoting $R = r_0 r_1$, we obtain the following equations at the carrier frequency and the two sidebands,

$$\begin{aligned}
\tilde{E}_1(\omega_l) &= t_0\tilde{E}_0(\omega_l) + R\tilde{E}_1(\omega_l)e^{-i\omega_l\tau} - \epsilon R\tilde{E}_1(\omega_l-\omega)e^{-i(\omega_l-\frac{\omega}{2})\tau} \\
&\quad + \epsilon R\tilde{E}_1(\omega_l+\omega)e^{-i(\omega_l+\frac{\omega}{2})\tau}, \\
\tilde{E}_1(\omega_l-\omega) &= t_0\tilde{E}_0(\omega_l-\omega) + R\tilde{E}_1(\omega_l-\omega)e^{-i(\omega_l-\omega)\tau} + \epsilon R\tilde{E}_1(\omega_l)e^{-i(\omega_l-\frac{\omega}{2})\tau}, \\
\tilde{E}_1(\omega_l+\omega) &= t_0\tilde{E}_0(\omega_l+\omega) + R\tilde{E}_1(\omega_l+\omega)e^{-i(\omega_l+\omega)\tau} - \epsilon R\tilde{E}_1(\omega_l)e^{-i(\omega_l+\frac{\omega}{2})\tau}.
\end{aligned} \tag{5}$$

In the above equations all sidebands higher than the first are neglected, since these come with the laser light contribution at $O((kx_o)^2)$ or higher. If $\tilde{E}_k$ stands for the following column vector,

$$\begin{pmatrix} \tilde{E}_k(\omega_l) \\ \tilde{E}_k(\omega_l-\omega_o) \\ \tilde{E}_k(\omega_l+\omega_o) \end{pmatrix} = \tilde{E}_k, \qquad k = 0,\ 1\ ; \tag{6}$$

then the above equations can be written in matrix form. We invert the matrix with the approximation $kx_0 << 1-R$, i.e. the frequency shift equivalent to the displacement of the mirror is much smaller than the line-width of the cavity (For high finesse cavities, the full-width at half maximum $\sim 2(1-R)$). Thus,

$$\tilde{E}_1 = \chi\tilde{E}_0, \tag{7}$$

where,

$$\chi = \begin{pmatrix} \frac{t_o}{1-Re^{-i\omega_l\tau}} & \frac{-t_o\epsilon Re^{-i(\omega_l-\frac{\omega}{2})\tau}}{(1-Re^{-i\omega_l\tau})(1-Re^{-i(\omega_l-\omega)\tau})} & \frac{t_0\epsilon Re^{-i(\omega_l+\frac{\omega}{2})\tau}}{(1-Re^{-i\omega_l\tau})(1-Re^{-i(\omega_l+\omega)\tau})} \\ \frac{t_0\epsilon Re^{-i(\omega_l-\frac{\omega}{2})\tau}}{(1-Re^{-i\omega_l\tau})(1-Re^{-i(\omega_l-\omega)\tau})} & \frac{t_o}{1-Re^{-i(\omega_l-\omega)\tau}} & 0 \\ \frac{-t_0\epsilon Re^{-i(\omega_l+\frac{\omega}{2})\tau}}{(1-Re^{-i\omega_l\tau})(1-Re^{-i(\omega_l+\omega)\tau})} & 0 & \frac{t_o}{1-Re^{-i(\omega_l+\omega)\tau}} \end{pmatrix}. \tag{8}$$

Since the input electric field E_0 is just at the carrier frequency, only the first column of the matrix is relevant and the intra-cavity field is a superposition of the fields at the carrier and the side band frequencies. Thus,

$$E_1(t) = [\chi_{11}e^{i\omega_l t} + \chi_{21}e^{i(\omega_l-\omega)t} + \chi_{31}e^{i(\omega_l+\omega)t}]\tilde{E}_0(\omega_l). \tag{9}$$

B. The static component of the intensity

The intensity of the laser beam at any point is obtained by taking the square modulus of the electric field at the point. The above equation gives the intracavity electric field $\tilde{E}_1$ at the corner mirror. At the end mirror,

$$\tilde{E}_1'(\omega) = \tilde{E}_1(\omega)e^{-i\omega\tau/2}, \tag{10}$$

where the ω could be $\omega_l, \omega_l \pm \omega$. The intensity can be broken up as a time-independent part I_{DC} and a time varying part $\delta I(t)$, which is due to the motion of the mirror. The first term in equation (9) gives I_{DC} where,

$$I_{DC}(\delta) = |\chi_{11}E_0(\omega_l)e^{-i\omega_l\tau/2}|^2 = \frac{{t_o}^2|E_o(\omega_l)|^2}{1-2R\cos(\delta)+R^2}, \tag{11}$$

where the phase offset $\omega_l \tau = \delta + 2n\pi$ has been introduced. Obviously, near resonance $\delta << 2\pi$. Eq. (11) is the usual Fabry- Perot curve with resonances at $\omega_l \tau$ equal to multiples of 2π. The full width at half maximum is $\simeq 2(1-R)$ when R is close to unity. The finesse of the cavity is $\mathcal{F} = \frac{\pi\sqrt{R}}{1-R}$. For Virgo the finesse is chosen to be about 50 [15] which corresponds to $R \sim 0.94$ and for LIGO the finesse is about 200 [16] ($R \sim 0.985$).

If we ignore time delay effects and assume that the intra-cavity power variation follows the static curve (that is, the motion of the mirror is slow compared with the timescale set by the storage time of the cavity $\tau_{stor} = \tau/(1-R)$) we can naively understand the nature of the problem when the radiation force is included. The radiation pressure force is $F_{rp} = 2I_{DC}A_{eff}/c$, where the intra-cavity power is $P_{DC} = I_{DC}A_{eff}$, A_{eff} is the effective area of the laser beam, and c is the speed of light $c \simeq 3 \times 10^8 ms^{-1}$. The restoring force of the pendulum is $-M\omega_p^2 x$, where $x = \delta/2k$ and ω_p is the natural pendulum angular frequency. In Figure (2) we plot the total force F_{tot}, and the corresponding potential, acting on the end mirror as a function of the displacement of the end mirror (for convenient parameters),

$$F_{tot} = 2I_{DC}A_{eff}/c - M\omega_p^2 x. \tag{12}$$

In figure(2a), the points where the curve cuts the $x-$axis are the multistable points (zero force). The slope of the curve at these points determines the stability. For a positive slope, any small displacement away from the equilibrium tends to take the end mirror further away and therefore these points are unstable; accordingly, the potential is maximal at these points. Whereas for the points at which the slope is negative, the force decreases and hence the mirror is brought back to equilibrium and therefore these points are stable (minimum of potential). For a larger power in the cavity more of these multistable points appear. As the finesse is increased, the magnitude of the slope is also increased (as the peak gets narrower) and the stability/instability becomes more pronounced.

C. The time dependent component of the intensity

For the time varying part of the intensity, we compute the expression,

$$\delta I(t) = \chi_{11}^* \chi_{21} |E_0|^2 e^{-i\omega(t-\tau/2)} + \chi_{11}^* \chi_{31} |E_0|^2 e^{i\omega(t-\tau/2)} + \text{c.c.} \tag{13}$$

The Fourier transform $\delta\tilde{I}(\omega)$ is then,

$$\delta\tilde{I}(\omega) = \frac{2it_o{}^2 R|E_o|^2 \epsilon \sin\delta e^{-i\delta_s}}{|1-Re^{-i\delta}|^2(1-Re^{-i(\delta+\delta_s)})(1-Re^{i(\delta-\delta_s)})}, \tag{14}$$

where, $\omega\tau = \delta_s$. The factor $\epsilon = kx_o$ contains x_o which can be related to the Fourier transform of the position of the mirror as, $\delta\tilde{x}(\omega) = x_o/2i$. We can obtain the power by just multiplying by the effective area A_{eff} and relate the Fourier component of the power to that of the position via a transfer function as,

$$\frac{\delta\tilde{P}(\omega)}{P_0} = \tilde{K}(\omega)\delta\tilde{x}(\omega), \tag{15}$$

where $P_0 = A_{eff}|E_0|^2$ is the input power. The expression for $\tilde{K}(\omega)$ using the above equations is,

$$\tilde{K}(\omega) = \frac{-4kRt_o{}^2 \sin\delta e^{-i\delta_s}}{|1-Re^{-i\delta}|^2(1-Re^{-i(\delta+\delta_s)})(1-Re^{i(\delta-\delta_s)})}. \tag{16}$$

This transfer function is derived with the restriction that the frequency drift related to the mirror displacement is much smaller than the line width of the cavity but there is no restriction on ω. However, we are interested in stability problems at frequencies lying in the band-width of the detector $\sim 10 - 2000$ Hz. In this regime we can obtain a simplifying approximation to the transfer function which then becomes a rational function. In the next subsection we obtain the simplified form.

D. Low frequency approximation of the transfer function

If we assume that $\omega\tau << 1$, i.e the fluctuations have a frequency ω much less than the free spectral range, then, keeping terms to second order in ω we get,

$$\tilde{K}(\omega) = -\frac{g(\delta)}{f(\Omega)}, \tag{17}$$

where Ω is a dimensionless frequency, and is defined in terms of the storage time τ_{stor}, or equivalently as a function of R and τ, as :

$$\Omega = \omega\tau_{stor} = \omega\tau/(1-R). \tag{18}$$

In the above equation $g(\delta)$ is like the envelope of the intensity change whereas $f(\Omega)$ is the dynamical part. The envelope is determined by the operating point δ and is appreciable only within the peak of the static curve. We have,

$$g(\delta) = \left[\frac{4kRt_0{}^2\sin\delta}{(1-R)^4(1+F\sin^2\delta/2)}\right]\left[\frac{1}{2R^2-R\cos\delta}\right], \tag{19}$$

$$f(\Omega) = \Omega_o^2 + 2i\lambda\Omega - \Omega^2, \tag{20}$$

where,

$$\begin{aligned} \Omega_o{}^2 &= \frac{1+F\sin^2\delta/2}{2R^2-R\cos\delta}, \\ \lambda &= \frac{R(\cos\delta - R)}{(1-R)(2R^2-R\cos\delta)}, \\ F &= \frac{4R}{(1-R)^2}. \end{aligned} \tag{21}$$

Inspecting $f(\Omega)$, we find that Ω_o is the frequency of oscillation of the intensity change whereas λ is proportional to the damping.

When $\Omega << \Omega_0$, we recover the static case. Then,

$$K(\Omega=0) = -\left[\frac{4kRt_0{}^2\sin\delta}{(1-R)^4(1+F\sin^2\delta/2)^2}\right] \equiv \frac{1}{P_0}\frac{dP_{DC}}{dx}, \tag{22}$$

where $P_{DC} = A_{eff}I_{DC}$ is the intra-cavity power.

Hence we see that, at low frequencies the intensity varies linearly with length (for small changes in length) with a proportionality constant being essentially the derivative of I_{DC} which is described by the static curve Eq. (11). At frequencies comparable to Ω_0, the transfer function resembles that of a damped harmonic oscillator with the strength of the response scaled by $g(\delta)$. This strength depends primarily on the operating point δ and is significant for values of δ within the peak of the static curve. To get some idea of the numbers involved we may use the Virgo finesse ($\mathcal{F} = 50$) which corresponds to $R = 0.94$. We can examine the case when the operating point is such that half of the maximum power is stored in the cavity, then, $\delta \sim \pm(1-R) = \pm.06$ (for the operational gravitational wave detectors δ will be smaller, typically less than a tenth of the half width at half maximum (HWHM) of the Airy peak [13,14]). For these parameters we get, $\Omega_o \sim 1.51$, $\lambda \sim 1.1$ and thus the period of oscillation and the damping time are of the same order. The time dependent intensity therefore oscillates like a critically damped harmonic oscillator with the time-scale of the storage time τ_{stor}.

III. COUPLING THE RADIATION PRESSURE TO THE MIRROR MOTION

In the previous section we calculated the response of the power to the time varying change in the cavity length which could be due to the motion of the mirror. In this section we perform the reverse computation of linking the power via the radiation pressure to the mirror motion and obtain a characteristic equation for the motion of the mirror. The forces acting on the mirror are firstly the radiation pressure force, secondly the gravity force which tends to restore the pendulum to equilibrium, and thirdly the force exerted by the locking servo loop installed to maintain the resonance. We must include the servo force in the model because no real suspended Fabry Perot cavity can even exist without it, and it would be physically meaningless to consider only a simple pendulum. The problem therefore must be solved self-consistently taking into consideration all these relevant interactions. It is assumed that the static radiation pressure force (due to P_{DC}) balances the spring restoring force at some point and we solve the equation of motion around this point.

The equation for the displacement of the mirror in the time domain is,

$$M(\ddot{x} + \gamma\dot{x} + \omega_p^2 x) = F_{rp}(t) + F_{servo}(t), \tag{23}$$

where $x(t)$ is the time-dependent displacement of the mirror near the equilibrium point, M, γ, and ω_p are the parameters of the pendulum suspension, namely, the effective mass, the damping coefficient and the natural angular frequency, respectively. It is more convenient at this juncture to switch over to the complex frequency domain via the Laplace transform and perform the analysis with the Laplace variable s which is linked to the real angular frequency ω by the relation $s = i\omega$. In the last section we discussed the radiation pressure force. In the next subsection we will discuss the servo-control and the reference transfer function given by Caron et al [14], in the context of the locking of the Virgo interferometer.

A. The servo loop

Since the bandwidth of the detector is typically between 10 Hz to few kHz , the servo control should be such that the motion of the mirror should be free in this range of frequencies while below 10 Hz the motion should be frozen. Let $G(s)$ be the transfer function of the pendulum suspension and $H(s)$ be the transfer function of the servo. Let x_{free} denote the free motion of the mirror, i.e. without the action of the servo and x_{out} the residual motion when the servo is connected in a feedback loop. Since the servo must also encounter the pendulum suspension, the product of the transfer functions $G(s)H(s)$ is actually effective (See Figure (3)). We have the following relation between the Laplace transforms,

$$x_{out} = \frac{x_{free}}{1 + GH} \tag{24}$$

and the x_{free} is related to the external force F_{ext} (in our case the radiation pressure force) by the relation,

$$x_{free} = GF_{ext}. \tag{25}$$

Between the various forces we have the following relations:

$$F_{total} = F_{ext} + F_{servo} = \frac{x_{out}}{G} = \frac{F_{ext}}{1 + GH}. \tag{26}$$

By the requirement mentioned above, we must have the gain $GH \sim 0$ in the bandwidth of the detector so that $x_{out} \sim x_{free}$. Secondly, below 10 Hz, GH should be large in order that the residual motion of the mirror is damped out i.e. $x_{out} << x_{free}$. Apart from this the transfer function is required to satisfy certain stability criteria, such as the Nyquist criterion and a phase margin of at least 45° at unit gain ($|GH| = 1$). The reference transfer function passes all these criteria. We describe the function below:

$$G = \frac{1}{M(s - s_1)(s - s_1^*)}, \tag{27}$$

$$H = H_0 \frac{(s - s_2)(s - s_2^*)(s - s_3)(s - s_3^*)}{s^2(s + 2\pi)(s - s_4)(s - s_4^*)}, \tag{28}$$

where the parameters have the following values: $H_0 = 2.24 \times 10^9 \mathrm{kg.sec}^{-3}, s_1 = 3.74(-10^{-6} + i)\,\mathrm{rad.s}^{-1}, s_2 = (-15. - 37.i)\,\mathrm{rad.s}^{-1}, s_3 = (-25. - 10.i)\,\mathrm{rad.s}^{-1}, s_4 = (-550. - 500.i)\,\mathrm{rad.s}^{-1}$. The transfer function has high gain at very low frequencies below 1 Hz, $|GH| \sim 10^6, 10^7$ and falls to unity at 22.2 Hz with a phase margin of about 45.5°. At high frequencies at about a kHz, the transfer function becomes negligible $\sim 10^{-3}$. The plot of the transfer function has been reproduced after [14] in Figure(4). We use this transfer function in our analysis henceforth, keeping the servo gain H_0 as a possible parameter.

B. The characteristic equation and the natural frequencies of the system

In this subsection we consider the full system of the radiation pressure force and the servo-control force acting on the suspended mirror with the position of the mirror and the motion of the mirror determining the instantaneous power and thus the radiation pressure. After Laplace transforming Eq. (22) or alternatively using Eq. (23) to Eq. (26) where F_{ext} is the radiation pressure force equal to $2\delta P(s)/c$, we obtain, from Eq. (15),

$$F_{ext}(s) = 2\frac{K(s)}{c}x_{out}(s). \tag{29}$$

Combining with Eq. (23) and (24) we get the characteristic equation for the system,

$$\frac{2}{c}K(s)G(s) = 1 + G(s)H(s). \tag{30}$$

With $s = i\omega = i\Omega/\tau_s$, where τ_s is an arbitrary time, we rationalise the above equation and write it in terms of the Laplace variable σ for which time is measured in units of τ_s. Although this is not strictly necessary, it avoids large numbers. (N.B. τ_s has nothing to do with the storage time of the cavity but has been chosen only for convenience). Setting $\sigma = \tau_s s$, the resulting equation is:

$$\begin{gathered}\sigma^2(\sigma+\sigma_0)(\sigma-\sigma_4)(\sigma-\sigma_4^\star)\sigma_{rp} + \\ \sigma^2(\sigma-\sigma_1)(\sigma-\sigma_1^\star)(\Omega_0^2+2\lambda\sigma+\sigma^2)(\sigma+\sigma_0)(\sigma-\sigma_4)(\sigma-\sigma_4^\star) + \\ k(\Omega_0^2+2\lambda\sigma+\sigma^2)(\sigma-\sigma_2)(\sigma-\sigma_2^\star)(\sigma-\sigma_3)(\sigma-\sigma_3^\star) = 0.\end{gathered} \tag{31}$$

The quantities appearing in the above equation have the following expressions:

$$\sigma_{rp} = \frac{2P_0 g(\delta)\tau_s^2}{Mc}, \tag{32}$$

$$k = \frac{H_0\tau_s^3}{M}, \tag{33}$$

$$\sigma_0 = 2\pi\tau_s, \tag{34}$$

$$\sigma_i = s_i\tau_s. \tag{35}$$

We have assumed here and in all the following that $\tau_s = 4\times10^{-4}$ sec. in the numerical expressions. The σ_i have the following values: $\sigma_1 \sim 1.5(-10^{-9}+i10^{-3}), \sigma_2 \sim -0.006-0.0148i, \sigma_3 \sim -0.01-0.004i, \sigma_4 \sim -0.22-0.2i$.

If we put $k = 0$ in the above equations we remove the action of the servo system. The parameter k essentially gives the gain of the servo, weighted by the mass of the mirrors. We will examine the $k = 0$ case later as a matter of interest.

The characteristic equation has real coefficients and is of degree 9 and has 9 complex roots, at least one of them real. In order that the system be stable, we must have the real parts of all the roots negative. However, the roots are functions of the parameters of the cavity. The most easily varied among these are the input power P_0, the operating point δ and the finesse determined through R. For the given transfer function of the servo these parameters can be varied within wide ranges and the roots then migrate in the complex plane. We however, do not study all the roots but investigate the migration of only two roots which have the tendency to 'cross over' into the right half $\sigma-$plane. To fix ideas, we list the values of the various quantities occurring in our calculations and also the roots for one typical set of the above parameters. For parameters corresponding to the Virgo example [15], namely mass $M = 28$ kg $R = 0.94$ (finesse of 50), and input power $P_0 \simeq 1$ kW (corresponding to the power recycling gain of about 100) and a phase offset $\delta \simeq -0.01$, we have $g(\delta) \simeq -10^{11}\mathrm{m}^{-1}, \sigma_{rp} \simeq 9.3\times10^{-5}, \Omega_0^2 \simeq 1.24, \lambda \simeq 1.13$. The roots in the $\sigma-$plane are the following: $-1.36, -0.91, -0.037, -0.18\pm0.16i, -0.01\pm0.005i, -0.0077\pm0.021i$. The following observations can be made for this example :

(i) Since all the roots have negative real parts, the system is stable for these values of the parameters.

(ii) The first two roots have moduli close to unity. This means that the power adjusts itself on the time scale of τ_s as the cavity length changes due to the motion of the mirror (not surprisingly since τ_s has been chosen in order to obtain numerical values near unity). These roots are basically governed by the transfer function $K(s)$.

(iii) However, it is the last two roots which decide the stability of the system, in the sense that increasing the input power or the finesse makes these roots migrate to the right-half of the $\sigma-$plane. For example, Figure (5) shows the behaviour of the real parts of the last two roots (only those for which the real parts can become positive), as the input power increases when $R = .94$ and $\delta = -.01$ are held fixed. We observe that it is only the last pair of the roots that cross over to the right half of the σ-plane. This is generally the case as has been borne out by extensive numerical computations, taking into account various values of the parameters, M, P_0, R, H_0 and δ.

We therefore, concentrate on these two roots and investigate how these roots cross the imaginary axis of the $\sigma-$plane as the parameters are varied.

C. The condition for stability

One must now examine Eq.(31) for the roots crossing over to the right half σ−plane. We consider three parameters, namely, the input power P_0, the reflectivity R and the operating point δ (plus eventually the mass M and the servo gain H_0) and hence one may expect regions in this 3-dimensional parameter space which correspond to stability/instability. However, we show below that a function κ of P_0, R and δ can be defined and the problem reduces to comparing the value of this function with a critical value of this parameter κ_{crit} which depends on the servo control transfer function. The function $\kappa(\delta, P_0, R)$ is essentially the scaled power. From the characteristic equation we make the following observations:

(i) The parameters δ, R, P_0, enter the coefficients through the quantities σ_{rp}, Ω_0^2 and λ; M appears in σ_{rp} and k, while H_0 only in k.

(ii) We find after extensive numerical scanning of the roots of this equation that the crossover of the two roots occurs near $i\Omega_{co} \sim \pm 0.023i$ (for $M \simeq 28$ kg) and hence when we are looking for the roots near this region the last two terms in the expression $\Omega_0^2 + 2\lambda\sigma + \sigma^2$ are small and can be neglected for this purpose. If the mass is less, the cross-over occurs for a slightly smaller value of Ω_{co} and the approximation is even better. We note that the servo gain has only a little influence on the value of Ω_{co} but affects the parameters (P_0, δ ...) for which the cross-over occurs. This brings down the degree of the equation from 9 to 7. More importantly it permits us to define the variable κ as follows:

$$\kappa(\delta, P_0, R) = \sigma_{rp}/\Omega_0^2 = \frac{2P_0 g(\delta)\tau_s^2}{\Omega_0^2 Mc}. \tag{36}$$

This lumps the three parameters of interest into κ and the problem simplifies considerably. Since at the cross-over σ is imaginary, Ω is real. We separate the real and imaginary parts of the characteristic equation each of which must vanish at the cross-over of the roots. We obtain the two equivalent equations in terms of the variable $u = \Omega^2$, and keep the first one, namely :

$$u^3 - \Big(\kappa + |\sigma_4|^2 - 2\sigma_0 Re(\sigma_4)\Big)u^2 + \Big((|\sigma_4|^2 - 2\sigma_0 Re(\sigma_4))\kappa - 2k(Re(\sigma_2) + Re(\sigma_3))\Big)u$$
$$+ 2k\Big(Re(\sigma_3)|\sigma_2|^2 + Re(\sigma_2)|\sigma_3|^2\Big) = 0 \tag{37}$$

We note that the last (constant) term is negative since the real parts of the s_i are all negative.

Since at the cross-over s should be purely imaginary, u must be real and positive. The roots obviously depend only on the one variable κ. We find that there exists a critical value κ_{crit} such that a real positive root exists when $\kappa > \kappa_{crit}$. In fact in Eq. (37), the cubic term can be neglected so that we have to deal only with a quadratic. Indeed, for the range of interest for the different parameters, κ_{crit} is found numerically to be about 10^{-4} to 10^{-3} and u^3 term can be dropped since this term is about 3 orders of magnitude smaller than the other terms. In the resulting quadratic κ_{crit} is obtained by setting the discriminant equal to zero and so we obtain a quadratic equation for κ_{crit}. Setting the *positive* expressions $\alpha_4 = |\sigma_4|^2 - 2\sigma_0 Re(\sigma_4)$, $\beta_{23} = -2k(Re(\sigma_2) + Re(\sigma_3))$ and $\gamma_{23} = -2k(Re(\sigma_3)|\sigma_2|^2 + Re(\sigma_2)|\sigma_3|^2)$, this equation is :

$$\alpha_4^2\kappa_{crit}^2 + 2(\alpha_4\beta_{23} - 2\gamma_{23})\kappa_{crit} + \beta_{23}^2 - 4\alpha_4\gamma_{23} = 0. \tag{38}$$

Solving, we find generally two negative roots κ_{crit} and κ'_{crit} and label them such that $\kappa_{crit} > \kappa'_{crit}$. For example in the case of relevant parameters for Virgo ($M = 28$ kg and $H_0 = 2.24 \times 10^9$ kg.s^{-3}), we find $\kappa_{crit} \simeq -6.18 \times 10^{-4}$ and $\kappa'_{crit} \simeq -3.34 \times 10^{-3}$. We find the same numerical values for constant ratios of H_0/M, since these two parameters enter in Eq.(38) through $k \propto H_0/M$. The quadratic form giving the discriminant of the simplified Eq.(37) as a function of κ has then a sign depending on the location of κ with respect to the two roots. As we want u to be real, the discriminant must be positive, giving $\kappa \geq \kappa_{crit}$ or $\kappa \leq \kappa'_{crit}$. However, in the second case, we find generally two real solutions for u but at least one of them negative, which is rejected since $u = \Omega^2$ is required to be positive for the stability of the system. The stability condition is finally $\kappa \geq \kappa_{crit}$. This condition is automatically fulfilled when $\delta > 0$, since in this case $g(\delta) > 0$ and then $\kappa > 0$, but it can be violated if $\delta < 0$. This immediately shows that for $\delta > 0$ the system is stable, just as in the free case (no servo) [8]. Only when $\delta < 0$ can the system be unstable.

1. Instability ($\delta < 0$)

In order to examine this case we write the function κ in more convenient variables.

We set $\Theta = 1 - R, \delta = \alpha\Theta$, since the operating point is more conveniently given in terms of the full width at half maximum $\simeq 2\Theta$ in these variables. In terms of Θ, the finesse $\mathcal{F}$ is given by $\mathcal{F} = \pi\sqrt{1-\Theta}/\Theta \simeq \pi/\Theta$, if $\Theta \ll 1$. Compared to unity we only keep terms to first order in Θ since normally Θ will be small compared to unity. From Eq. (36) we obtain the following expression for $\kappa(\alpha, P_0, \Theta)$:

$$\kappa(\alpha, P_0, \Theta) = \frac{\alpha(1+\alpha^2-3\Theta)(1+1.5\Theta)}{(1+\alpha^2)^3\Theta^2}\frac{32\pi\tau_s^2}{\lambda M c}P_0. \tag{39}$$

The condition for stability $\kappa > \kappa_{crit}$ then becomes,

$$-\frac{\alpha(1+\alpha^2-3\Theta)(1+1.5\Theta)}{(1+\alpha^2)^3\Theta^2}P_0 < \frac{\lambda M c}{32\pi}\frac{|\kappa_{crit}|}{\tau_s^2}. \tag{40}$$

The equality between the left and right terms in this equation gives the equation of the curve separating the stable and unstable domains in the space of parameters. Given the finesse, the mass and κ_{crit}, we can write for example the critical input power P_{crit}, above which instability occurs, as a function of the detuning δ :

$$P_{crit} = \frac{\lambda M c}{32\pi}\frac{|\kappa_{crit}|}{\tau_s^2}\frac{(1+\alpha^2)^3\Theta^2}{\alpha(1+\alpha^2-3\Theta)(1+1.5\Theta)}, \tag{41}$$

which can be re-casted as:

$$P_{crit} = P_{char}\frac{(1+\alpha^2)^3\Theta^2}{\alpha(1+\alpha^2-3\Theta)(1+1.5\Theta)}, \tag{42}$$

where we have defined the characteristic power P_{char} by :

$$P_{char} = \frac{\lambda M c}{32\pi}\frac{|\kappa_{crit}|}{\tau_s^2} \simeq 340\left(\frac{M}{28\text{kg}}\right)\left(\frac{\lambda}{1064\text{nm}}\right)\left(\frac{|\kappa_{crit}|}{6.18\times10^{-4}}\right)\text{kW}. \tag{43}$$

In the case of relevant parameters for Virgo ($M = 28$ kg and $\lambda = 1064$ nm) [15] and $|\kappa_{crit}| \simeq 6.18 \times 10^{-4}$, we have $P_{char} \simeq 340$ kW. In the case of LIGO ($M = 10.7$ kg and $\lambda = 1064$ nm) [16] and for a similar servo transfer function as for Virgo, we find $|\kappa_{crit}| \simeq 2.85 \times 10^{-3}$ and we have then $P_{char} \simeq 600$ kW, while for the same servo transfer function except that the gain is chosen so that the ratio H_0/M is the same as in Virgo ($|\kappa_{crit}| \simeq 6.18 \times 10^{-4}$), we have $P_{char} \simeq 130$ kW. The figure(6) is a plot of the critical input power P_{crit} as a function of the phase detuning from resonance δ for various finesses in the case of Virgo mirrors ($M = 28kg$). Above each critical curve, the system is unstable and below it is stable. We first note the existence of a minimum at $\delta = \Theta$, which is at HWHM of the Airy peak. This minimum can be explained by noting that at HWHM the derivative of the power with respect to δ is maximum, so the radiation pressure force is also maximal (see Eq.(22)). Secondly, we see that with a planned finesse of 50 and an input power about 1 kW (circulating power inside the recycling cavity), the arm cavities of Virgo are always stable, whatever the operating point. However, increasing the power in the recycling cavity and/or increasing the finesse of the arm cavities can produce instabilities. For example, for a operating point at $\delta = \Theta/10$ (tenth of the HWHM), the Virgo cavities can become unstable for a power in the recycling cavity of about 10 kW, corresponding to an improvement of a factor $\sqrt{10} \simeq 3$ of the shot noise, with respect to the nominal configuration (1 kW in the recycling cavity). The case of LIGO does not seem more problematic, as it would be in the non-servoed case, due to the lighter mirrors. Figure (7) shows the critical power as a function of δ for a cavity having a finesse of 200 and 10.7 kg mirrors as in LIGO and two servo gains corresponding to $|\kappa_{crit}| \simeq 2.85 \times 10^{-3}$ (same gain as in Virgo) and $|\kappa_{crit}| \simeq 6.18 \times 10^{-4}$ (same ratio gain/mass as in Virgo). Except for the gain, the servo system is assumed to be the same as in the Virgo case, although this could not be the case, due to different designs for the seismic isolation and so to different sensitivities at low frequencies. However, we assume the servo loop transfer function for LIGO to be the same as for Virgo, merely to get an idea of the order of magnitude for the various parameters. If the servo gain is designed such that the ratio gain/mass is the same as in Virgo, the figure (plain curve) shows instability domains for input powers as low as about 100 W. In the case of LIGO, the circulating power inside the recycling power should be of the order of 300 W (with a laser power of 6 W and a recycling power gain about 50) [17], so that an operating point near a tenth of the HWHM could be possibly unstable. However, an increase of the gain (dashed curve) by a factor less than 3, allows to recover stability. In any case, in future improved versions of LIGO/Virgo, unstable domains could be theoretically removed by an increase of the servo gain, but, in practice, this gain can not be increased indefinitely, due to limitations in the electronics. So, we must keep in mind the possible occurence of instabilities for some range of operating points, depending on the optical configuration and on the design of the servo loops. Finally we want

to emphasize that, if the powers in LIGO/Virgo should have to be increased, even moderately (say by a factor $\sim$ 10), and even if the locking point is closer to the perfect resonance ($\delta = 0$) (so that the "static" operating point is stable), the domain around the HWHM inducing possible instabilities, some trouble could occur during the lock acquisition, when the detuning of the cavities becomes near the HWMW. Clearly, this can have serious implications for the "proto-locking" procedure and this problem needs further investigation.

2. *Switching off the servo*

When the servo is switched off, the only other force acting on the mirror besides the radiation pressure is gravity. As in the previous case for $\delta > 0$ there is no instability but for $\delta < 0$, instability can occur at very small input powers because the only force now counteracting the radiation pressure is gravity. Again the $\Omega << 1$ approximation is applicable and setting $\kappa = 0$ in Eq. (31), we obtain the following equation for the characteristic frequency σ:

$$(\sigma - \sigma_1)(\sigma - \sigma_1^*) + \kappa = 0 \tag{44}$$

Neglecting the damping in the pendulum, the equation becomes,

$$\sigma^2 + |\sigma_1|^2 + \kappa = 0 \tag{45}$$

The solutions are of the form $e^{\sigma t/\tau_s}$ and hence for κ zero or positive the system is stable. This corresponds to the operating point $\delta \geq 0$. When $\kappa < 0$ corresponding to $\delta < 0$ there can be instability when $|\kappa| > |\sigma_1|^2$. In terms of critical input power this means,

$$P_{crit} = \frac{|s_1|^2 M c \Omega_0^2}{2|g(\delta)|}, \tag{46}$$

for instability to occur. For typical parameters of the Virgo interferometer, and for an operating point chosen at one tenth of the HWHM ($\delta = -6 \times 10^{-3}$), the critical input power is about 50 W. In the case of LIGO, for the similar operating point ($\delta = -1.5 \times 10^{-3}$) the critical input power is even lower, about 2.5 W, due to lighter mirrors and higher finesse cavities.

IV. CONCLUSIONS

We have analysed the effect of radiation pressure in laser interferometric cavities with freely hanging mirrors, which are locked by a servo-control feedback loop. We have assumed the transfer function for the servo given by Caron et al. [14] which satisfies the usual stability criteria. After performing the analysis we find that stability depends on the input power, the finesse, the mass of the mirrors, the servo gain and the operating point of the cavity. We find that instability can only occur if $\delta < 0$ (where δ is the phase offset from resonance). For a given $\delta < 0$, and a given servo gain, mass and a certain value of the finesse, there is a critical input power over which the system becomes unstable. The system tends to be unstable for high finesses/high powers. We derive an analytic relation between the input power, finesse, mass, operating point and a parameter depending on the ratio gain/mass, which decides between stable and unstable situations.

The main result is that for a finesse of 50 (which applies to Virgo), the cavity always exhibits stability for recycling powers of a few kW. For a finesse of 200 (which applies to LIGO), with the same input powers(for a few kW), we find that instability may occur. This will have some implications for the design of the servoloop transfer function. It will therefore be of importance to investigate the stability of LIGO cavities with an appropriate servo transfer function since such high powers are expected to be present in the advanced detectors of the future. Indeed, the shot noise is likely to limit the sensitivity of LIGO/Virgo at least above some hundreds of Hz, so an improvement of the sensitivity of these detectors in the future demands a decrease in the shot noise level. However the shot noise level decreases only as the square root of the power stored in the recycling cavity. This implies that to reduce the shot noise by one order of magnitude, we need to increase the powers by two orders of magnitude. Clearly, the radiation pressure effects can play an important role in improved versions of LIGO/Virgo, and particular care must be dedicated, especially, to the design of the servo loops.

In this work we have considered the displacement of the mirror to be very small. In particular the movement of the mirror is within a fraction of the linewidth of the cavity. For much larger powers, it might be important to consider larger displacements, in which case the equations become nonlinear and simulations may have to be performed in order to gauge the stability of the system.

We have not considered in this problem any tilt of the mirror, due to the radiation pressure. A small tilt of the mirror will introduce higher order modes into the cavity. The radiation pressure, will now couple these different modes. It will be therefore important to investigate the nature of the coupling and possible oscillations, if any. We also plan to investigate the effects of input laser noise on the stability of the cavity.

ACKNOWLEDGMENTS

This work has been supported by the Indo-French Center for Promotion of Advanced Research (IFCPAR), project 1010-1.

---

[1] K. S. Thorne, in *in 300 Years of Gravitation*, edited by S. W. Hawking and W. Israel (Cambridge Univ. press, Cambridge, 1987) p. 330.
[2] *The Detection of Gravitational Waves* edited by D. Blair (Cambridge University Press, Cambridge, 1991).
[3] A. Giazotto, Phys. Rep. **182**, 365 (1989)
[4] R. W. P. Drever, in *Gravitational Radiation*, edited by N. Deruelle and T. Piran (North-Holland, Amsterdam, 1983).
[5] J.-Y. Vinet, B. J. Meers, C. N. Man, A. Brillet, Phys. Rev. D **38**, 433 (1988).
[6] A.Dorsel et al., Phys. Rev. Lett. **51**, 1550 (1983).
[7] P. Meystre et al., J. Opt. Soc. Am. **B2**, 1830 (1985).
[8] N. Deruelle and P. Tourrenc, *Gravitation, Geometry and Relativistic Physics* (Springer, Berlin, 1984); J. M. Aguirregabiria and L. L. Bel, Phys. Rev. A **36**, 3768 (1987); P. Tourrenc and N. Deruelle, Ann. Phys. Fr. **10**, 241 (1985).
[9] B. J. Meers and N. MacDonald, Phys. Rev. A **40**, 3754 (1989).
[10] V. V. Kulagin and V. N. Rudenko, Phys. Lett. A 214, 123 (1996).
[11] P. Hello and J-Y. Vinet, J. Phys. (France) **51**, 2243 (1990).
[12] S. V. Dhurandhar, P. Hello, B. S. Satyaprakash and J-Y. Vinet, "On the stability of giant cavities in interferometric gravitational wave detectors", accepted for publication in Applied Optics (1996).
[13] R. Flaminio and H. Heitmann, Phys. Lett. A **214**, 112 (1996).
[14] B. Bourdas, B. Caron and F. Marion, Virgo note NTS006 (1994); B. Caron et al., "A preliminary study of the locking of an interferometric for gravitational wave detection", accepted for publication in Astroparticle Physics (1996).
[15] Virgo Final Design, unpublished (1995, updated 1997).
[16] A. Abramovici et al., Science **256**, 325(1992).
[17] D. Shoemaker (MIT-LIGO team), private communication (1997).

FIG. 1. The electric fields in a Fabry Perot cavity with front mirror reflectivity r_0 and a suspended end mirror with reflectivity r_1.

FIG. 2. (a) A schematic, depicting the force experienced by the end mirror versus the displacement. (b) The corresponding potential. Points (1), (2) represent respectively unstable and stable equilibrium.

FIG. 3. A schematic indicating the servo loop. G:Pendulum suspension transfer function, H:servo transfer function, F_{ext}:the force due to the radiation pressure, x_{out}:the total displacement of the mirror, x_{free}:the displacement of the mirror without the servo.

FIG. 4. A plot of $|GH|$ (the product of the pendulum suspension and servo transfer functions) verses the frequency in Hz.

FIG. 5. Migration of the real parts of the relevant roots towards the half-plane $Re(\sigma) > 0$, as the input power increases. The other parameters are fixed : $H_0 = 2.24 \times 10^9$ kg.s^{-3}, $M = 28$ kg, $R = 0.94$ and $\delta = -0.01$. Here instability arises for am input power about 8 kW.

FIG. 6. The critical input power P_{crit} (in kW) versus the cavity phase detuning δ in the case of a Virgo-like configuration : $H_0 = 2.24 \times 10^9$ kg.s^{-3}, $M = 28$ kg, but for different finesses. With a finesse of 50, and a power in the recycling cavity typically about 1kW, the Virgo arm cavities are always stable, whatever δ is. We see also the influence of the finesse : if the finesse would have to be increased, everything else being constant, instability could occur for finesse above 100.

FIG. 7. The critical input power P_{crit} (in kW) versus the cavity phase detuning δ in the case of a LIGO-like configuration : $M = 10.7$ kg, $R = 0.985$ (finesse about 200). The two curves correspond to two servo loop gains. Plain curve : same gain as in figure (6) : $H_0 = 2.24 \times 10^9$ kg.s^{-3}. Dashed curve : $H_0 = 0.86 \times 10^9$ kg.s^{-3}, corresponding to the same ratio H_0/M as in figure (6). We see clearly the action of the gain.

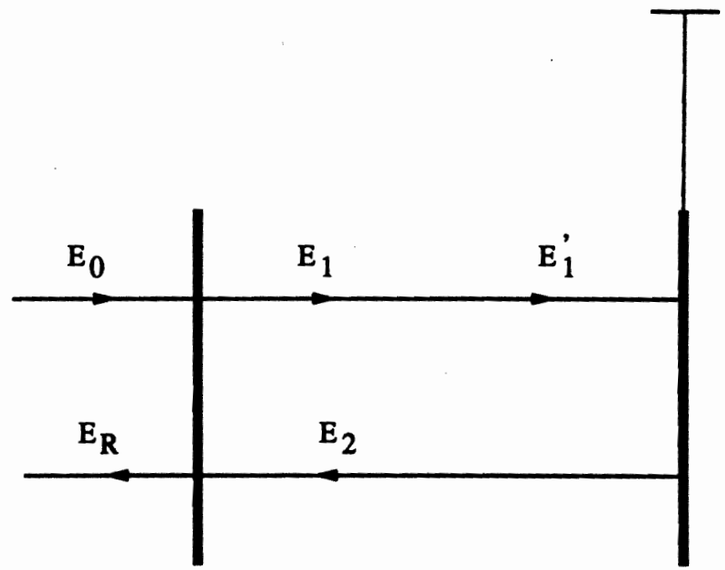
E_0
E_1
E_1'
E_R
E_2

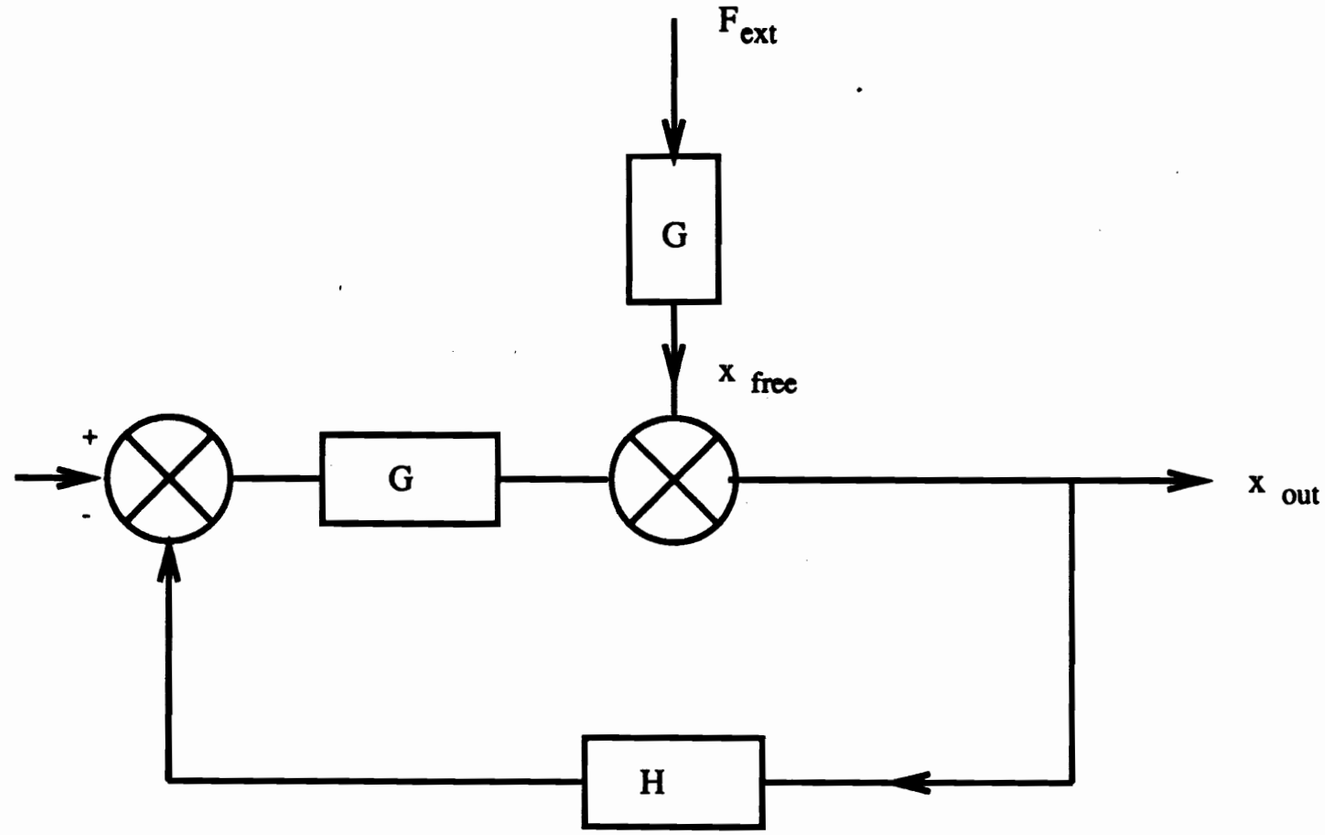
F ext
G
x free
+
-
G
x out
H

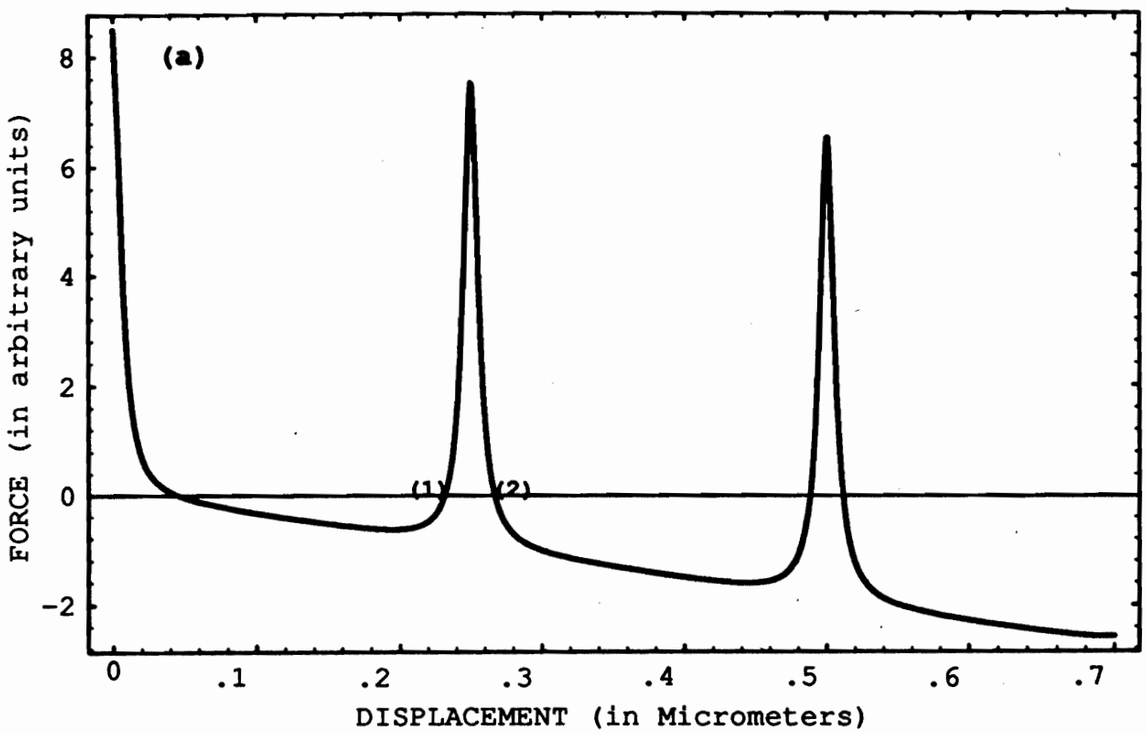
(a)
FORCE (in arbitrary units)
8
6
4
2
0
-2
(1)
(2)
0
.1
.2
.3
.4
.5
.6
.7
DISPLACEMENT (in Micrometers)

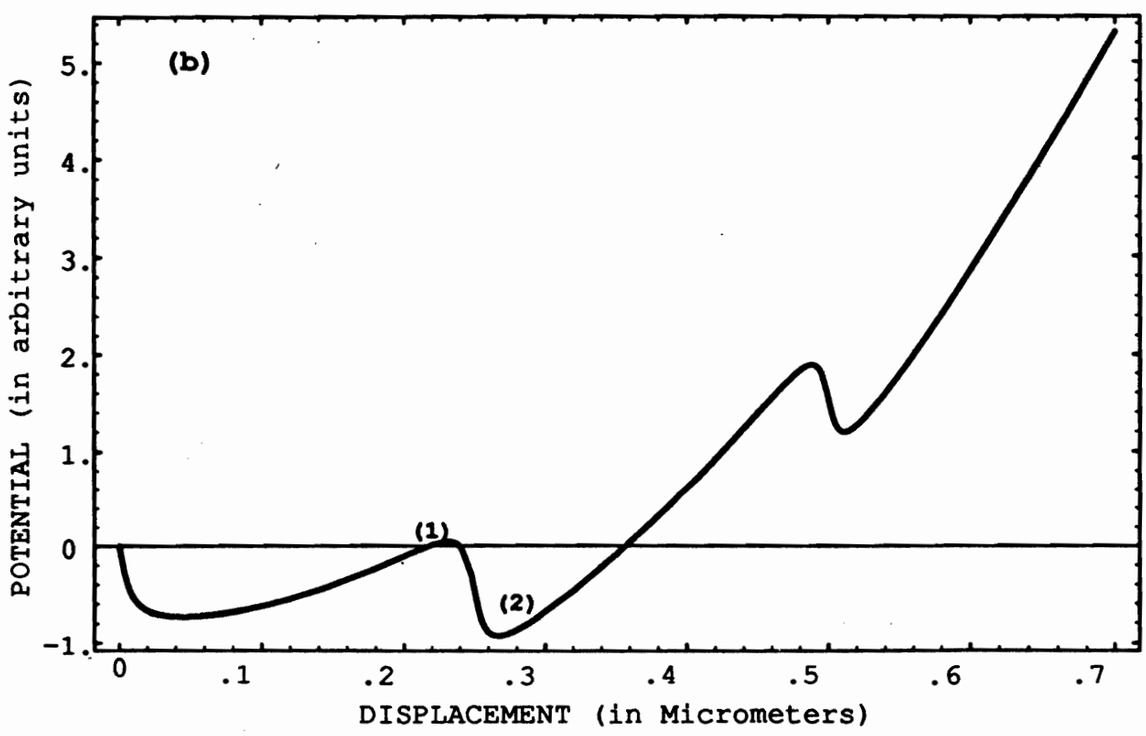
(b)
POTENTIAL (in arbitrary units)
5.
4.
3.
2.
1.
0
-1.
(1)
(2)
0
.1
.2
.3
.4
.5
.6
.7
DISPLACEMENT (in Micrometers)

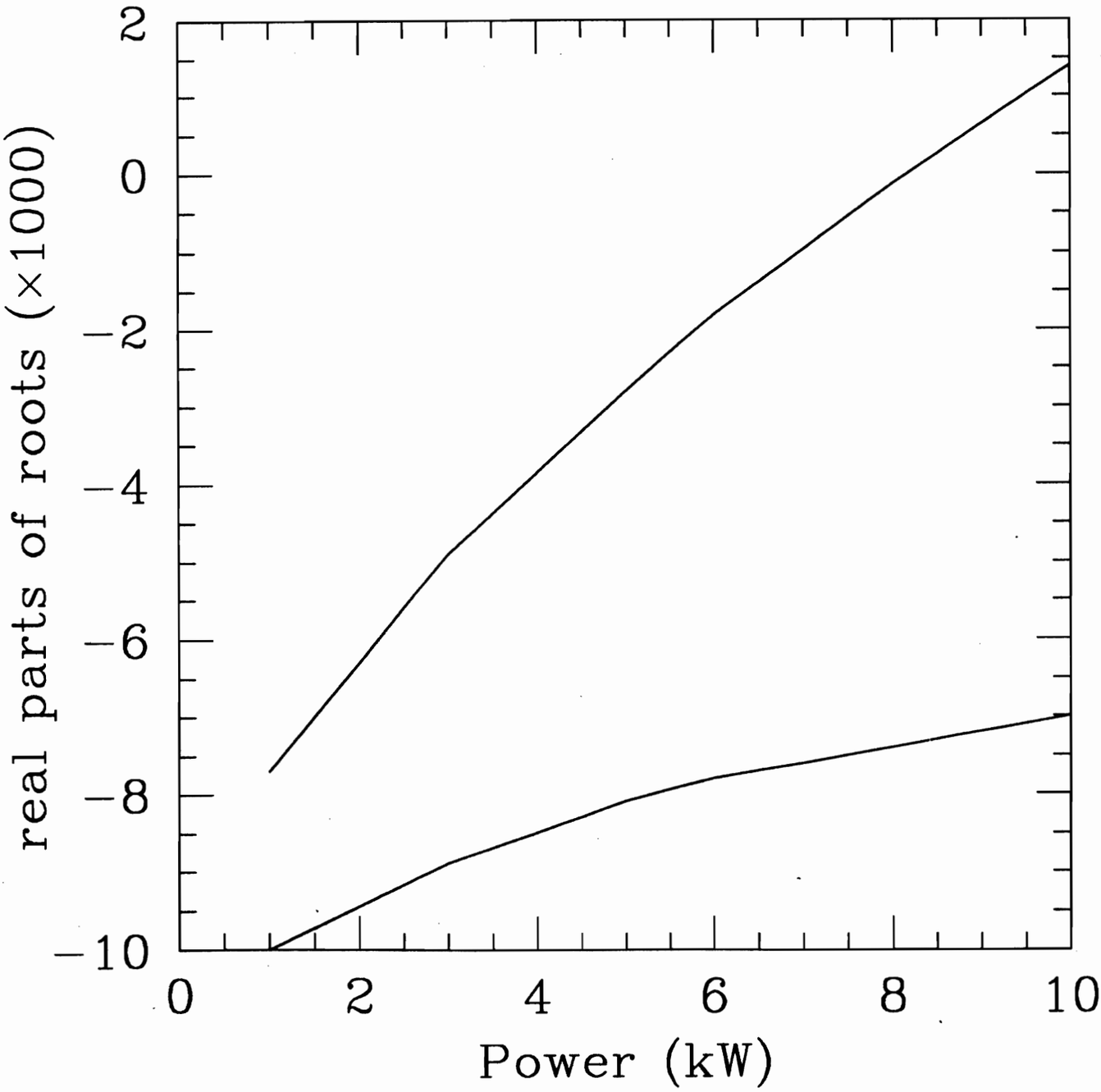
2
0
−2
−4
−6
−8
−10
real parts of roots (×1000)
0
2
4
6
8
10
Power (kW)

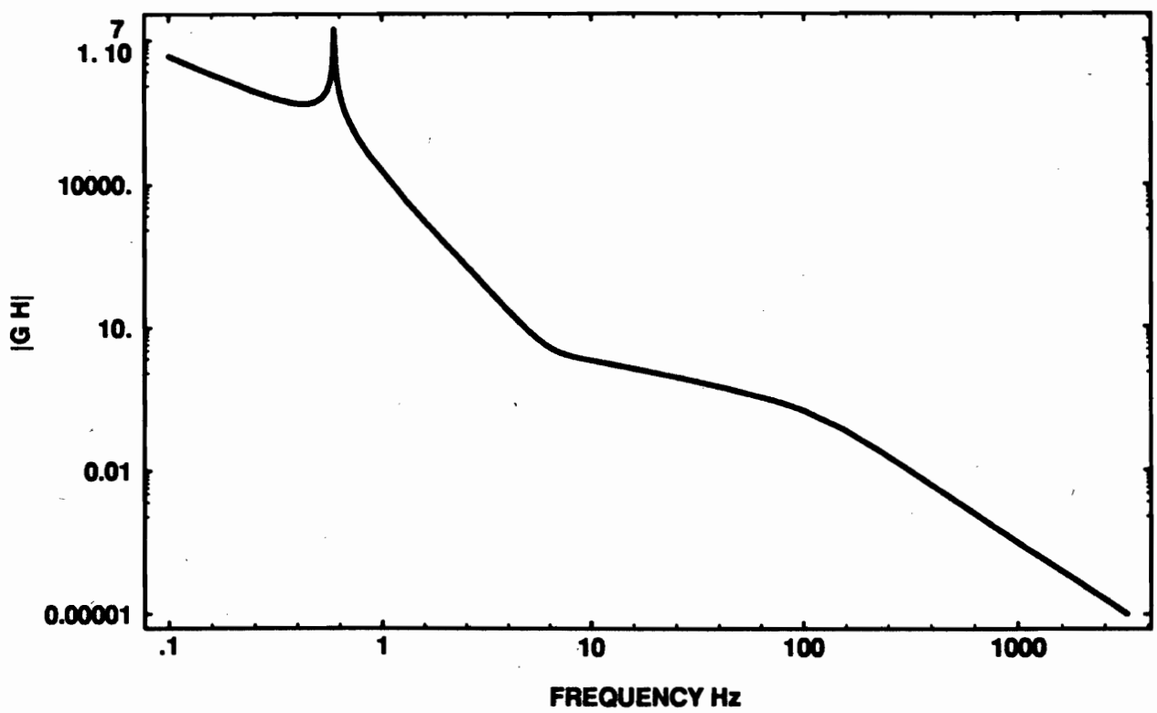
7
1. 10
10000.
10.
0.01
0.00001
|G H|
.1
1
10
100
1000
FREQUENCY Hz

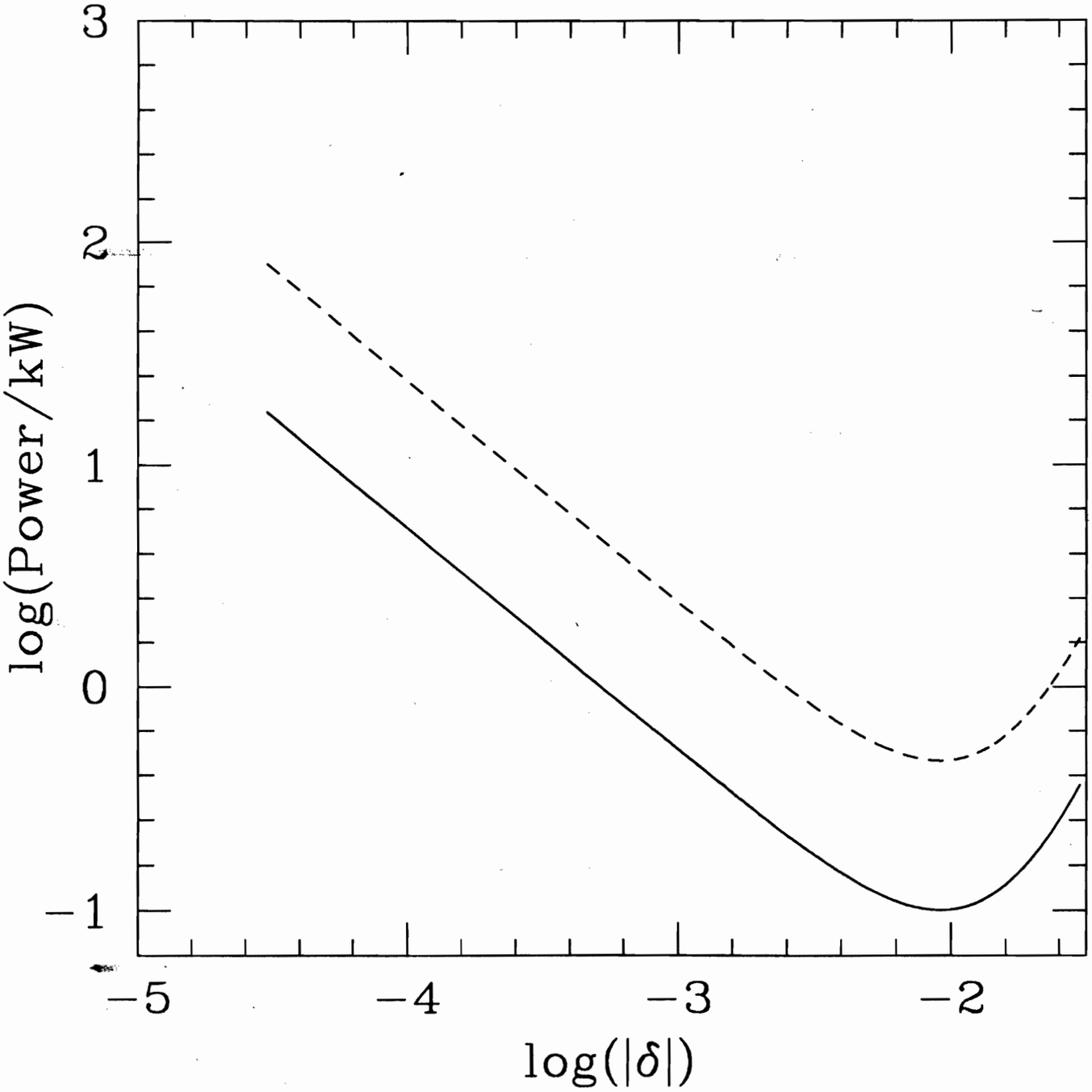
3
2
1
0
−1
log(Power/kW)
−5
−4
−3
−2
log(|δ|)

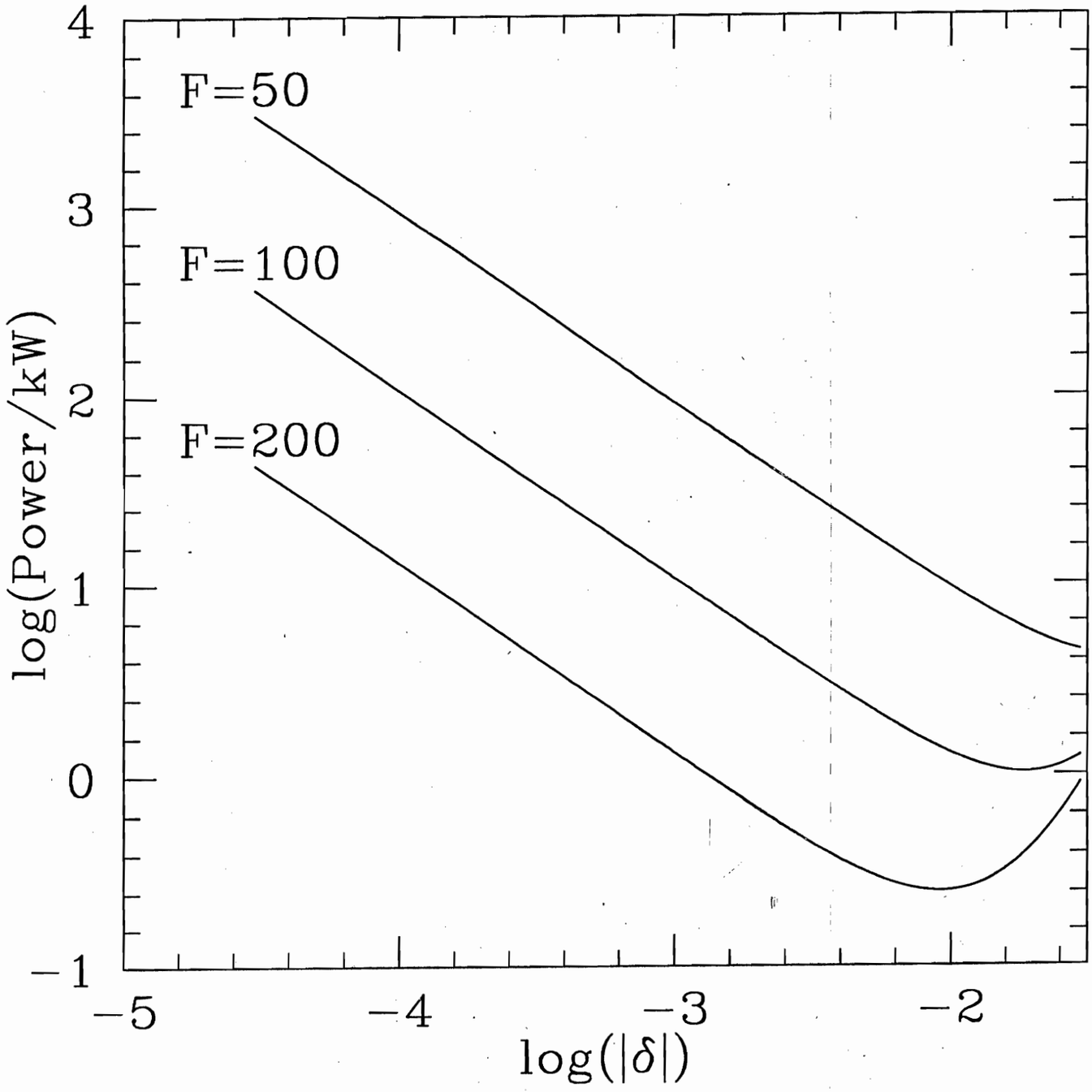
F=50
F=100
F=200
log(Power/kW)
log(|δ|)
4
3
2
1
0
−1
−5
−4
−3
−2